The prediction method of entrainment rate by breakup of large drop during reflood in a TH code

Seung Hyun Yoon, Kyung Doo Kim, Jaeseok Heo, Kwiseok Ha*
Korea Atomic Energy Research Institute, 111, Daedeok-daero 989beon-gil, Yuseong-gu, Daejeon, Republic of Korea.
**Corresponding author: ksha@kaeri.re.kr*

1. Introduction

Large droplet occurs with a high flow rate of water during a reflood phase in loss of coolant accidents. As a preliminary study [1], we introduced the very simple method to deal with the breakup of a large droplet and entrainment from the large droplet to a small droplet for inverted slug flow regime. For this paper, we described more realistic method to predict the entrainment, which is proper to a transient phenomenon. Using SPACE code with verified breakup and entrainment models, we improved calculation results of the wall temperature and steam mass flow rate measured at outlet for a high flooding case as expected.

2. Implementation and verification

2.1. Determination of large droplet size by breakup model

The original version of SPACE considered the shape of the large droplet in the ISF regime as an elliptic. It determined the size of the major axis as equation (1), which is the same approach as MARS-KS:

$$D = \sqrt{\alpha_D} D_h \quad (1)$$

where D denotes the large droplet and α_D indicates the large droplet fraction.

To address the breakup and the size change of the large droplet in a physical way, we referred to the research of Lee-NO [2]. They suggested constitutive equations for the breakup of the maximum stable droplet size (D_{stable}) and the Sauter mean diameter for small droplets through the validation of experimental data. They also verified that the models were applicable to the 1-D calculation. The essential equations are followed as:

$$\frac{dD}{dt} = -\frac{D - D_{stable}}{\tau} \quad (2)$$

$$D_{stable} = \begin{cases} \dfrac{\sigma_D^{\,2}}{\rho_g (v_g - v_D)^3 \mu_g} & \text{for stripping breakup} \\ We_{critical} \dfrac{\sigma_D}{\rho_g (v_g - v_D)^2} & \text{for bag breakup} \end{cases} \quad (3)$$

$$\tau = \begin{cases} 20 \dfrac{D/2}{(v_g - v_D)} \sqrt{\dfrac{\rho_D}{\rho_g}} & \text{for stripping breakup} \\ \pi \sqrt{\dfrac{\rho_D (D/2)^3}{2\sigma_D}} & \text{for bag breakup} \end{cases} \quad (4)$$

$$\frac{dv_D}{dt} = \frac{3}{4} \frac{\rho_g}{\rho_D} \frac{(v_g - v_D)^2 C_D}{D} \quad (5)$$

$$\frac{d_{32}}{D} = \frac{1}{(1 + ae^{1/4\delta^2})} \quad (6)$$

where τ is the duration time for an unstable large droplet, ρ is the density , σ is the surface tension, v is the velocity, d_{32} is Sauter mean diameter for small droplets, a is the ratio of the volume median diameter to the maximum stable diameter, and δ is the distribution parameter. The critical Weber number is set as 12.

When the current size of the large droplet is bigger than the maximum stable size for the stripping breakup, D_{stable} and τ are calculated with the values for stripping breakup in equations (3) and (4). If D is between D_{stable} for the stripping and bag breakups, the result will be obtained by the parameters of the bag breakup. These equations will be implemented and verified in the SPACE in the following paragraphs.

It should be noted that equations (2) ~ (6) are based on a Lagrangian approach. Since SPACE is made from the Eulerian system with a staggered grid (Fig. 1), the represented size of the large and small droplets in a face (i.e. grid for velocity) and a cell (i.e. grid for scalar values such as the temperature, pressure, etc.) has to be specified.

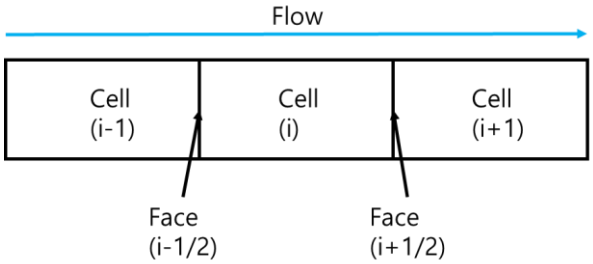

Fig. 1. Schematic for the Eulerian system.

We determined the large droplet size at the face with the initial conditions of the vapor and the large droplet in the previous cell until the large droplet from the cell reached the face through iterations:

$$D_{i-1/2,t_1} = -\frac{\Delta t}{\tau_{i-1/2,t_0}}(D_{i-1,t_0} - D_{i-1/2,stable,t_0}) \quad (7)$$
$$D_{i-1/2,t_n} = -\frac{\Delta t}{\tau_{i-1/2,t_{n-1}}}(D_{i-1/2,t_{n-1}} - D_{i-1/2,stable,t_{n-1}}) \ \ when\ n>1$$

where the subscript with i indicates the index in Fig. 1, t_0 is the initial timstep, and t_n is the n-th timestep.

The large droplet size of a cell was calculated with the three steps: 1) Calculate the breakup result of the incoming large droplet from the inlet face for the one-time step, 2) Obtain the breakup result from the own cell by using the drop size at the previous time, and 3) Calculate the mass-averaged value with the results of the first and second steps:

$$D_{i,t_1,1} = -\frac{\Delta t}{\tau_{i,t_0}}(D_{i-1/2,t_0} - D_{i,stable,t_0})$$
$$D_{i,t_1,2} = -\frac{\Delta t}{\tau_{i,t_0}}(D_{i,t_0,f} - D_{i,stable,t_0}) \quad (8)$$
$$D_{i,t_1,f} = \frac{m_{i-1/2}D_{i,t_1,1} + (m_i - m_{i+1/2})D_{i,t_1,2}}{m_{i-1/2} + m_i - m_{i+1/2}}$$

where the subscript f means the final value.

To confirm and verify the implementation, we calculated and compared the large droplet size in terms of the Eulerian method (equation (8)), and the Sauter mean diameter in a cell counting all the droplets' information from the Lagrangian method (equation (9)). The number of large droplets (n_D) were sustained over a distance [3].

$$D_{32} = \frac{\sum n_D D^3}{\sum n_D D^2} \quad (9)$$

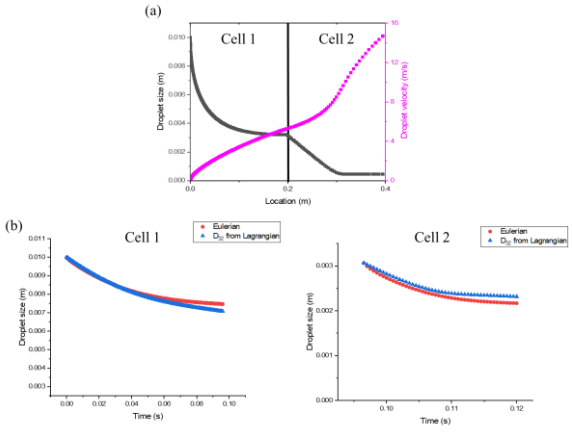

Fig. 2. (a) The distribution and velocity of large droplets in two cells from Lagrangian method (b) Large droplet size vs. time in each cell (v_g = 40 m/s, p = 2.8 bar).

Fig. 2 consisted of both stripping and bag breakups. As shown in Fig. 2 (a), the stripping breakup occurs in Cell 1, and the droplet experienced the bag breakup in Cell 2. The initial droplet reached the end of Cell 1 at the simulation time of 0.965 s. Therefore, the time frame of Cell 2 began in 0.965 s. The average discrepancies between Eulerian and D32 from Lagrangian in each cell were 1.98 % and 4.25 %, as described in Figure 3 (b). The results of Figs. 2 and 3 indicate that the behaviors of a large droplet estimated in an Eulerian cell agreed well with the Lagrangian method, even without tracking all of the droplets' information.

2.2. Entrainment model development by breakup of large droplets

We combined two methods to obtain the proper entrainment: One is defined as a simple method, and the other is defined as a transient method.

The simple method is an appropriate logic to the steady-state condition. Assume that the droplet size changes from D_0, D_1, D_2, … D_n in the certain domain. When the inlet mass of large droplets (m_{D_0}) is constant, the entrainment mass is saturated at the n-th time step value as follows:

$$m_{E,simple} = m_{D_0}(1 - \frac{D_n^3}{D_0^3}) \quad (10)$$

where m_E is the entrainment mass.

However, this simple method has the possibility to overestimate the entrainment before the droplet really reaches the outlet face. To predict the entrainment at an early transient, we summed the entrainment from the inflow breakup at the inlet face and from the breakup of the mass-averaged droplet in a cell during the one-time step as the following equation:

$$m_{E,transient} = m_{D_0,t_0}(1 - \frac{D_{i,t_1,1}^3}{D_{i-1/2,t_0}^3}) + m_{D_{cell},t_0}(1 - \frac{D_{i,t_1,f}^3}{D_{i,t_0,f}^3}) \quad (11)$$

Finally, we took the minimum value between the simple and transient methods as follows:

$$m_{E,final} = \min(m_{E,simple}, m_{E,transient}) \quad (12)$$

To verify the results of equation (12) compared to the Lagrangian method, we calculated with the conditions of a steam velocity of 40 m/s and the pressure of 2.8 bar.

In Fig. 3, the upper graph and lower graph illustrate the results of cell 1 and cell 2, respectively. As depicted in Fig. 3, the suggested approach (i.e., the green triangle) that takes the minimum value between the simple method and the transient method shows good agreement compared to the results tracking all of the droplets' entrainment (i.e., the black rectangle). The average deviations were within 2.24 ~ 4.77 %. Summarizing the results in this section, we successively verified the suggested method to calculate the droplet size and entrainment for the structure of the system code.

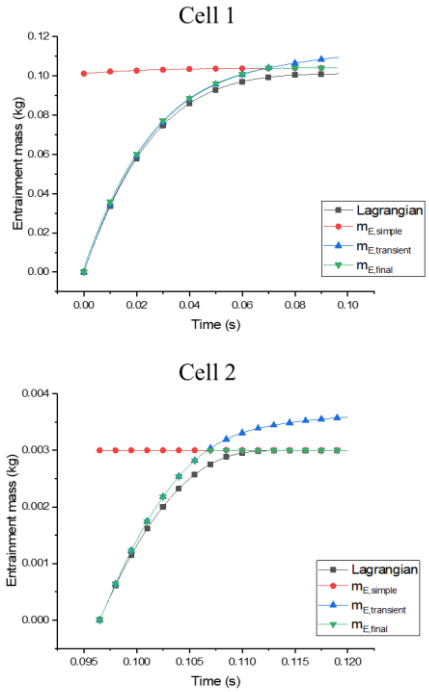

Fig. 3. (a) The distribution and velocity of large droplets in two cells from Lagrangian method (b) Large droplet size vs. time in each cell (v_g = 40 m/s, p = 2.8 bar).

3. Assessment results and discussion

There is no clear criterion to distinguish the low and high flooding rates in refloods. We selected 2 experimental cases which have relatively high injection velocities in FLECHT-SEASET [4], as described in Table I.

Table I: Assessment matrix

Parameters	FS-31701	FS-31302
Flooding rate (mm/s)	155.0	76.5
Pressure (MPa)	0.28	0.28
T_{sub} (K)	78.2	79.2
Initial rod peak power (kW/m)	2.3	2.3

We compared the steam mass flow rate at the outlet, and the wall temperature showing the PCT and the quenching temperature.

Fig. 4 shows the steam mass flow rates with the time after the beginning of the refloods. To compare the prediction accuracies quantitatively, we used the software [5] that contained the Fast Fourier Transform Based Method (FFTBM). For the original and modified results for SPACE, the average amplitudes showed 0.477 and 0.349 (FS-31701), 0.457 and 0.305 (FS-31302), respectively. The improvements in predicting the steam flow rate were achieved by the vaporization for the additional entrainment generated from the breakup of the large droplets in the modified SPACE.

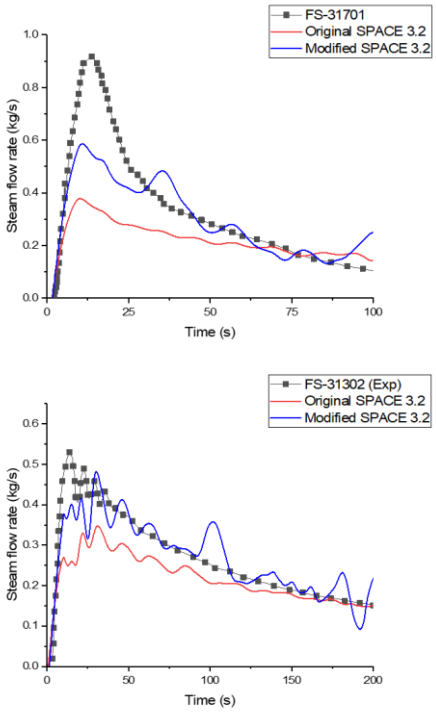

Fig. 4. Steam mass flow rate at the outlet vs. time for FS-31701 and FS-31302.

Table II: AAs for the wall temperature of FS-31701

Locations	Original	Modified
1.22 m	0.094	0.087
1.83 m	0.235	0.175
2.44 m	0.227	0.118

Table III: AAs for the wall temperature of FS-31302

Locations	Original	Modified
1.22 m	0.074	0.098
1.83 m	0.186	0.097
2.44 m	0.177	0.098

As described in Tables II-IIII and Figs 5-6, the overall trend for wall temperatures for each location was improved.

4. Conclusions

We implemented the phenomena induced with the large droplet, which was produced at the ISF regime and has been roughly described in conventional codes. As we assessed SPACE after modifications, we noted that the predictions for the steam mass flow rate, and the wall temperatures (including the PCT and the quenching temperature) were generally improved.

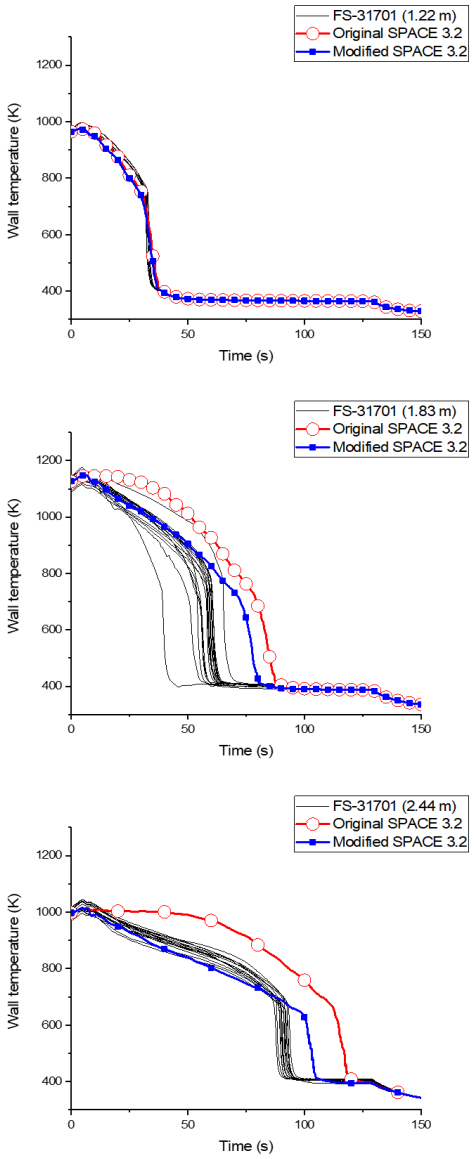

Fig. 5. Wall temperature vs. time for FS-31701

REFERENCES

[1] Yoon, S. H., Kim, K. D., Ha, K., & Lee, S. W. The effect of droplet breakup model for reflood experiments with a high flooding rate. KNS 2019 Fall.

[2] Lee, S. W. & No, H. C. Droplet size prediction model based on the upper limit log-normal distribution function in venturi scrubber. Nucl. Eng. Technol. (2019). doi:10.1016/J.NET.2019.03.014

[3] Chou, W. H. and G. M. Faeth. 1998. “Temporal Properties of Secondary Drop Breakup in the Bag Breakup Regime.” International Journal of Multiphase Flow 24(6):889–912

[4] N. Lee, S. Wong, H. Yeh, and L. Hochreiter, "PWR FLECHT SEASET unblocked bundle, forced and gravity reflood task data report," Electric Power Research Institute, EPRI. NUREG/CR-2256, 1981.

[5] Heo, J. and K. D. Kim, 2015, "PAPIRUS, A Parallel Computing Framework for Sensitivity Analysis, Uncertainty Propagation, and Estimation of Parameter Distribution." Nuclear Engineering and Design, 292, pp237-247.

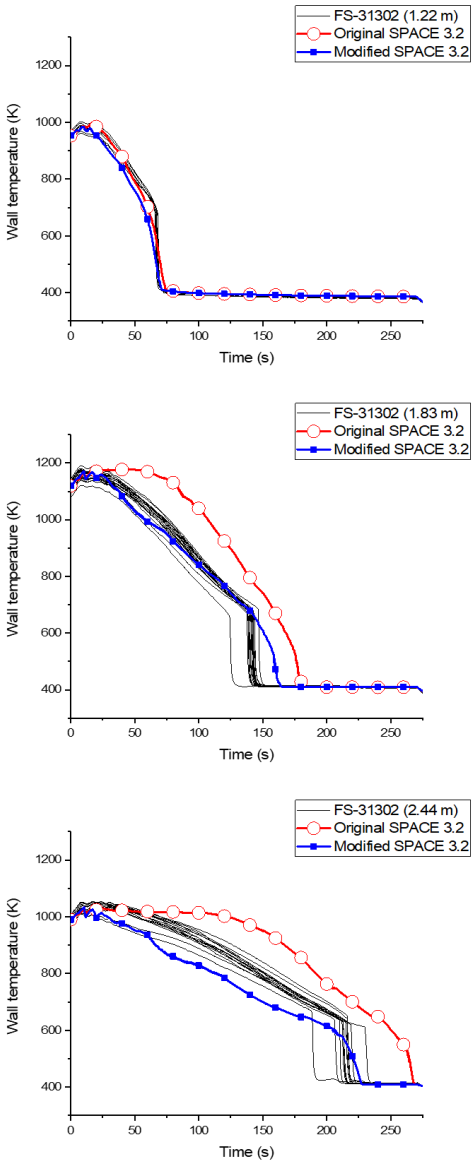

Fig. 6. Wall temperature vs. time for FS-31302